LA-UR- 03-2391

Approved for public release; distribution is unlimited.

36

Title: MEASUREMENT OF STRAIN HEAT IN SHOCK-LOADED 304 STAINLESS STEEL: IMPLICATIONS TO POWDER CONSOLIDATION; ORAL PRESENTATION OF FULL PAPER

Author(s): Karl P. Staudhammer

Submitted to: DYMAT 2003, Porto, Portugal, September 8 - 12, 2003

LOS ALAMOS NATIONAL LABORATORY
3 9338 01038 5275

Los Alamos National Laboratory, an affirmative action/equal opportunity employer, is operated by the University of California for the U.S. Department of Energy under contract W-7405-ENG-36. By acceptance of this article, the publisher recognizes that the U.S. Government retains a nonexclusive, royalty-free license to publish or reproduce the published form of this contribution, or to allow others to do so, for U.S. Government purposes. Los Alamos National Laboratory requests that the publisher identify this article as work performed under the auspices of the U.S. Department of Energy. Los Alamos National Laboratory strongly supports academic freedom and a researcher's right to publish; as an institution, however, the Laboratory does not endorse the viewpoint of a publication or guarantee its technical correctness.

Form 836 (8/00)

Abstract. Over the past decades there have been numerous papers on the shock response of materials and more specifically towards metal powder compaction and consolidation. In general, the shock process for powdered materials has utilized the traditional pressure-volume shock relationships proportioned to the initial packing densities of the powders. However, this approach and its resulting data are in controversy due to the lack of knowledge of its associated particle strain and strain temperature uncertainties. This paper will describe the current understanding as well as the experimental technique used to obtain the shock response for distended materials. The above parameters are described within a pressure-strain-temperature interdependence. It was found that the experimentally measured strain heat was not only a function of initial packing density but also a function of powder size and distribution.

1. INTRODUCTION

When metal specimens are shock compressed, nearly all the work of plastic deformation is converted into heat. This heat, at high shock rates is deposited in the sample and there is insufficient time for this heat to dissipate out of the shocked sample. Thus, the temperature will increase proportional to the magnitude of the strain. There are a number of parameters that dictate the dominance of this temperature. Attempts to define this overall temperature is still ongoing. This more so particularly for distended (powder) materials, as they have a loss of porosity and an increase of the apparent density. This loss of porosity is achieved through deformation (strain) and at strain rates of ~10^6/sec. results in an increase in residual temperature.

It has long been argued that in explosive compaction/consolidation that a great deal of the generated energy is consumed at the surface of the powder particles, which leads to much higher temperatures at these surfaces and in many cases causing melting. Thus, by these means, individual particles can be welded together. Additionally, little attention has been given to the powder morphology and particle size in shock compression studies of distended materials. This is attributed to a larger extent to the investigations by Boade [1] who studied nominally spherical copper powders having narrow size distributions and average particle sizes of 10, 50, and 100 μm, found no differences in their Hugoniots. Similarly, the Hugoniots determined by Butcher and Karnes [2] for iron powders. Also, Gourdin [3] concluded that if the effects on initial packing densities are taken into account, that the shock properties per se are not a strong function of powder morphology or particle size.

Observations such as these have thus lead to defining the shock Hugoniot of a distended system as the shock Hugoniot of the full density of the base metal proportioned to the distended density. For the shock Hugoniot this is a very good approach in that the energy deposition is within the shocked system. This however, assumes that the energy deposition is in fact uniform through out the system, which cannot be true if the energy deposition is at the interstices of the powder particles. Thus, for powders having the same density of packing but differ in particle size, their energy distribution at the interstices along with the contributed strain energy must be different.

2. BACKGROUND

When a strong shock wave propagates into a solid homogeneous material, the microstructure is altered. Additionally a significant amount of strain can also occur depending on the amount of deformation. Great efforts are made to eliminate this strain, however, this is in fact very difficult to obtain and for the most part is achieved by minimizing this strain. However, for distended materials an added amount of deformation occurs in the powder compaction/consolidation process, which is strongly influenced by the initial density [3]. What has not been recognized in the assessment of density is the fact that, theoretically, different mono-sized particles have the same densities but not the same deformation upon compaction/consolidation. This happens in spite of the fact that their shock Hugoniots are the same.

In considering the total energy input into a consolidated monolith, or simply the temperature, one obtains the following: $\Delta T(\text{Overall}) = T_o(\text{Initial temperature}) + \Delta T(\text{Residual temperature}) + \Delta T(\text{Strain})$, wherein the $\Delta T(\text{Strain})$ has two components for a distended system, these being $\Delta T(\text{Overall sample strain}) + \Delta T(\text{Void collapse})$. To varying degrees, each of these terms are controllable. The overall driving force is to keep the total temperature increase of the sample below the melting temperature of the distended material. Non-the-less, some temperature is needed for consolidation. Thus, in controlling temperature, one may vary the initial temperature (T_o), as it is the easiest by either heating or cooling the sample prior to shock loading. An appropriate pressure must be chosen which is sufficient for bonding but not excessive and similar for the residual temperature by controlling the amount of overall and local strain.

Shock compaction/consolidation of distended materials have been described by many investigators as very viable if one processes within a region wherein consolidation is optimum. This window of opportunity is a strong function of the variables discussed above. All of these variables in a shock environment have either a direct or indirect contribution to the overall temperature. To better understand the shock consolidation process, it behooves one to understand not only the source of the temperature, but its temperature-time relationships and how it affects the consolidation process.

3. SHOCK EXPERIMENTS

To delineate and obtain information on these various temperature contributions an experimental investigation of shock compaction/consolidation that was based in part on the Mach stem lens formation work by C. E. Morris, R. G. McQueen and S. P. Marsh [4]. One of

the fortuitous aspects of the cylindrical implosion design is its suitability as a screening tool with controllable strain and its very high success rate of recovery. The designs allow the experimenter to observe in one shot a wide variety of pressure and strain variables necessary to characterize optimum compaction/consolidation as a function of initial temperature, initial powder densities as well as mono-sized constant density experiments. Previous investigations [5] have shown the effectiveness of this technique using 304 SS powders. It should be emphasized that the powder was selected to help in modeling of the formation of the mach stem zone (over compacted) and that this technique is not particularly used or recommended to compact powders for monolithic use due to the gradation of pressure and strain variations along the axial length of the samples produced. But rather as a screening technique to define the shock parameters, packing densities and concomitant effect of powder size.

The shock loading assembly is shown in fig.1. This design and its modified versions are discussed in several papers [4, 6-8]. The pressure at the top is approximately 12 GPa and increases to 109 GPa at the bottom of the holder for an initial density of 68% at the central axis. As the powder density changes, the magnitude of the pressure "seen" by the powder also changes. These densities are shown in fig. 2. Hydrocode computer calculations were employed to determine the shock pressures experienced by the powder. These calculations employed a two-dimensional Eularian code, which has the ability to incorporate multi-materials, material strengths, equation-of-state, and programmed burn rate for the high explosives. A radial pressure profile at an axial length of 39 mm is shown in fig. 3 for a powder having an initial density of 68%. At this axial position, the 304 SS powder experiences a pressure from 54 GPa at the outer edge of the sample holder to a maximum of 109 GPa at the central axis.

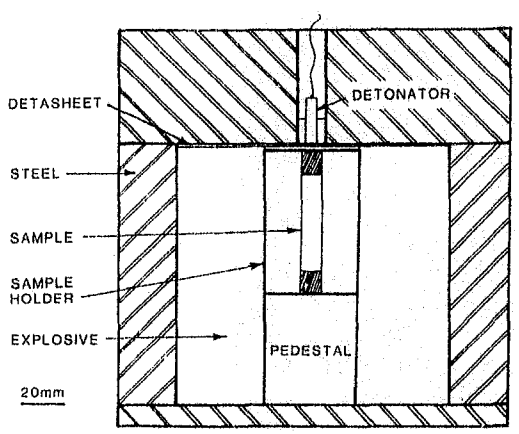

Figure 1 Schematic of shock loading design.

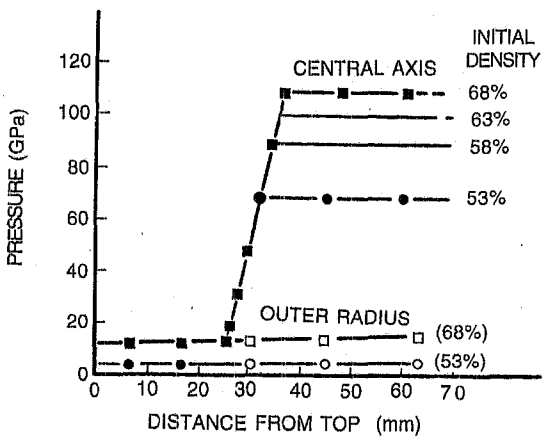

Figure 2 Hydrocode calculations of achieved pressure vs. axial length as a function of initial density.

4. RESULTS

A cross section schematic of a post shocked 304 SS specimen holder is shown in fig. 4. Of the initial densities investigated (58, 63, 68%) all had similar characteristics to that shown in

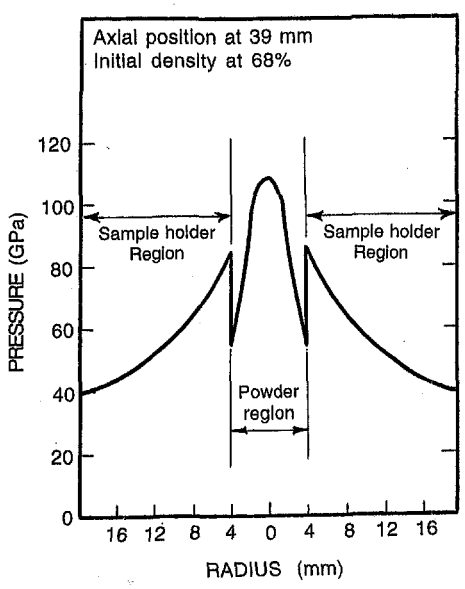

Figure 3 Calculated pressure vs. radial position in the powder sample.

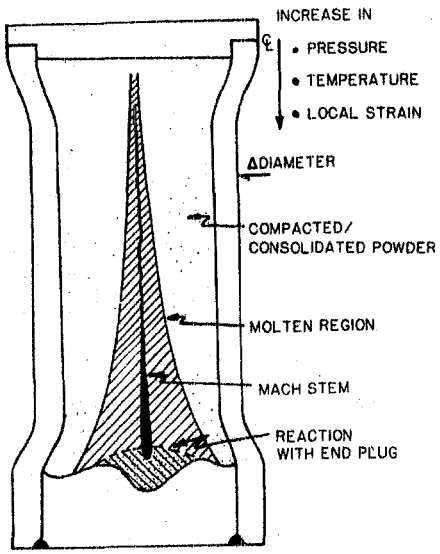

Figure 4 Cross section schematic of cylindrical 304 SS sample showing post-shocked characteristics.

fig. 4, only variations in magnitude were observed. For example, for lower initial density greater melting and greater decrease in diameter were noted as compared to the higher initial density samples. In the consolidation of these 304 SS powders the region of interest is outside the central crosshatched region in fig. 4. The further one moves radially out from any axial length position, the less consolidation is observed and essentially only compaction at the extreme edges of the holder. Figure 5 is a micrograph of the cross section of what is depicted schematically in fig. 4. This observation is illustrated in fig. 6 for four axial length positions (the sample holder was cut at these axial length positions). Each axial length position has a maximum pressure that the 304 SS powder had experienced at its central axis (left vertical axis of fig. 6). With an increase in radial distance, these pressures drop off, and reflect the same profile as shown in the central portion of fig. 4. Observations of post shocked samples sectioned at axial lengths of 10.2, 17, 21, and 39 mm revealed the melt zone to follow line A-A′ in axial and radial space all contained pressure-temperature conditions, which resulted in total melting of the 304 SS powders. Below line A-A′ regions of consolidation and compaction were observed. It should be noted that this figure only illustrates the above-mentioned regions for 68% initial density. As the initial density changes (over some limited range, the profile (shape) of A-A′ curve will change along with the concomitant pressure achieved. In so doing, several samples with varying initial densities were prepared and shocked under the same conditions. Observations of melt, consolidation and compaction were made, similar to that shown in fig. 6. The results of all of these observations are shown in fig. 6. Instead of plotting axial length position and radial distance, pertinent primarily to the test technique used here, fig. 7 shows the compaction, consolidation, and melting regimes achieved at any given pressure for specific packing densities of the 304 SS powder. The initial density range varied from 53 to 68%.

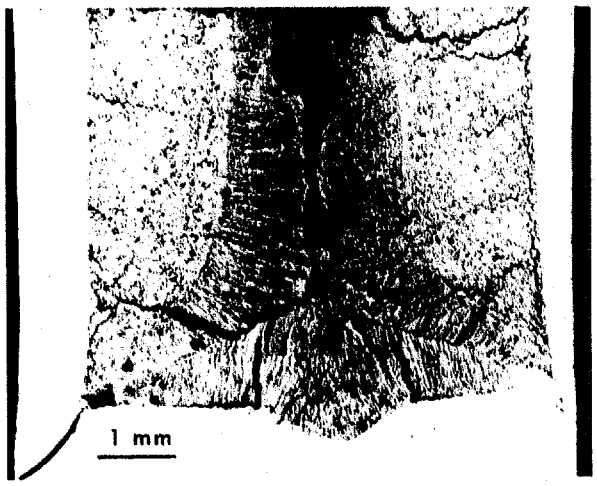

Figure 5 Micrograph of cross section of the lower portion of the shock compacted 304 SS powder, initial density 68%.

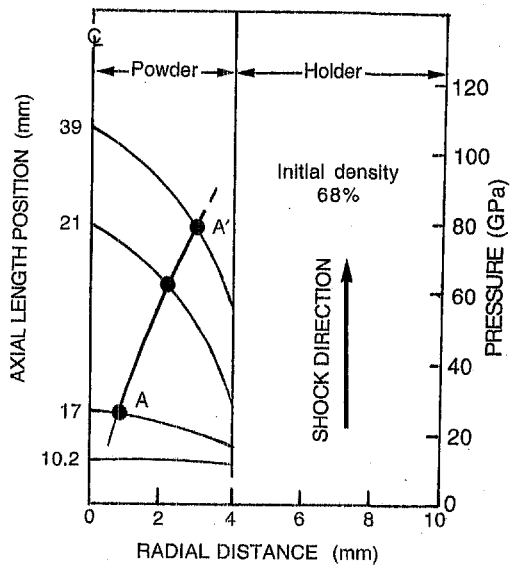

Figure 6 Pressure vs. radial distance (from centerline C) for selected axial length positions of 10.2, 17, 21, and 39 mm in a 304 SS powder having an initial density of 68%. The 39 mm axial length corresponds to the right half of the powder region in figure 3.

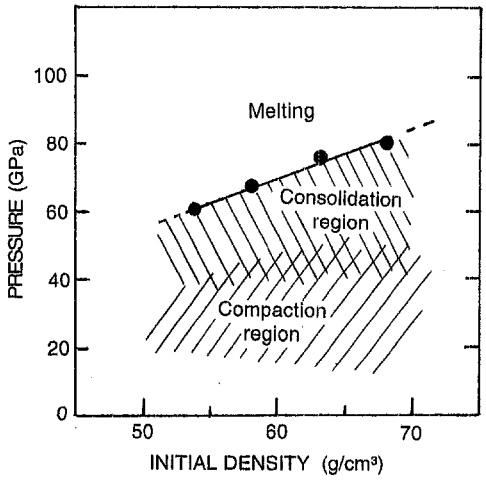

Figure7 Pressure vs. initial density of the 304 SS. The shaded areas indicate regions of compaction and consolidation. Melting results for pressures, which are above the curve.

The increase in the melt zone radius with increased travel of the shock wave is not surprising in light of the increase in pressure and a change from primarily surface deformation of particles at low pressures, to more massive non-homogeneous particle deformation at higher pressures. This is indicative of an increasing entropic temperature as well as adiabatic heating resulting in a large melt zone. This melt zone is more prominent at

the lower densities than at the higher densities. This is due to the greater local particle strain for the lower density as described in [9]. The Mach stem zone (neglecting edge effects) as shown in fig. 4 dose not exceed 0.8 mm radius along the central axis and is consistent with the Mach stem region calculated in the hydrocode calculations. The melt zone, however, is not accounted for in the hydrocode calculations. Focusing on local strains that are obtained from powder void collapse and its associated temperature must also be dealt with. For mono-sized powders, the number of contact points per unit volume greatly increases with a decrease of powder size. The residual temperature after consolidation is primarily an accumulation of localized heating within the void regimes as a result of local straining to fill void space. Thus, the void volume increases, the local particle strain would be expected to increase correspondingly, and an increase in the local residual temperature occurs.

5. SUMMARY

In using the shock loading geometry described here along with the two-dimensional hydrocode, one is able to define in one experiment (i.e., fixed density and given powder size) the loci of pressure for optimal consolidation. In addition, local thermal effects that are produced during shock consolidation have been presented and illustrated above. Many earlier developed theories and models have been proposed that account for the deposition of energy (temperature) uniformly on the outer surface of each particle. From the arguments and observations presented here, it is clear that melting where it occurred was localized and occurred at regions of greatest strain (i.e. to fill the void), and not uniformly distributed through out the particle surfaces. It was demonstrated that the residual melt fraction increased with void volume for powders that had equivalent initial packing densities. While the shock Hugonoit appears not to be affected for similar densities achieved by small or large particles, the resultant temperature distribution within the shock consolidation, however, is not uniform. It is different for consolidation of small and large particle sized powders. Consequently, the resulting monolith (bulk) will have variations within the microstructure and as such needs to be accounted for.

References

[1] Boade R. R., J. Appl. Phys. 41, (1970), 4542-4551.

[2] Butcher B. M. and Karnes C. H., J. Appl. Phys. 40, (1969), 296-2976.

[3] Gourdin W. H., Progress in Matls. Sc., 30, (1986), 39-80.

[4] Morris R. G., McQueen R. G. and Marsh S. P., Shock Waves in Condensed Matter-1983, Proc. of the APS Topical Conference, Santa Fe, New Mexico, 1983, (North Holland, 1984), 207.

[5] Johnson K. A. and Staudhammer K. P., "EXPLOMET 85," Eds. L. E. Murr, K. P. Staudhammer and M. A. Meyers, (Marcel Dekker, New York, NY, 1986), 525-542.

[6] Johnson K. A., Murr L. E. and Staudhammer K. P., Acta Metall., 33, (4), (1985), 677-684.

[7] Staudhammer K. P., Johnson K. A. and Olinger B., Shock Waves in Condensed Matter, Eds. , J. R. Asay, R. A. Graham and K. Straub, (Elsevier Sci. Pub., 1983), 419-424.

[8] Staudhammer K. P. and Johnson K. A., Impact Loading and Dynamic Behavior of Materials, May 1987, (Informationsgesellshaft mbH, Verlag, Germany, 1988), 839-844.

[9] Staudhammer K. P. and Murr L. E., in Industrial Applications of Shock Waves, Chp. 7, Ed. L. E. Murr, (Noyes Publications, New Jersey, USA, 1988), 237-264.